Figure S1

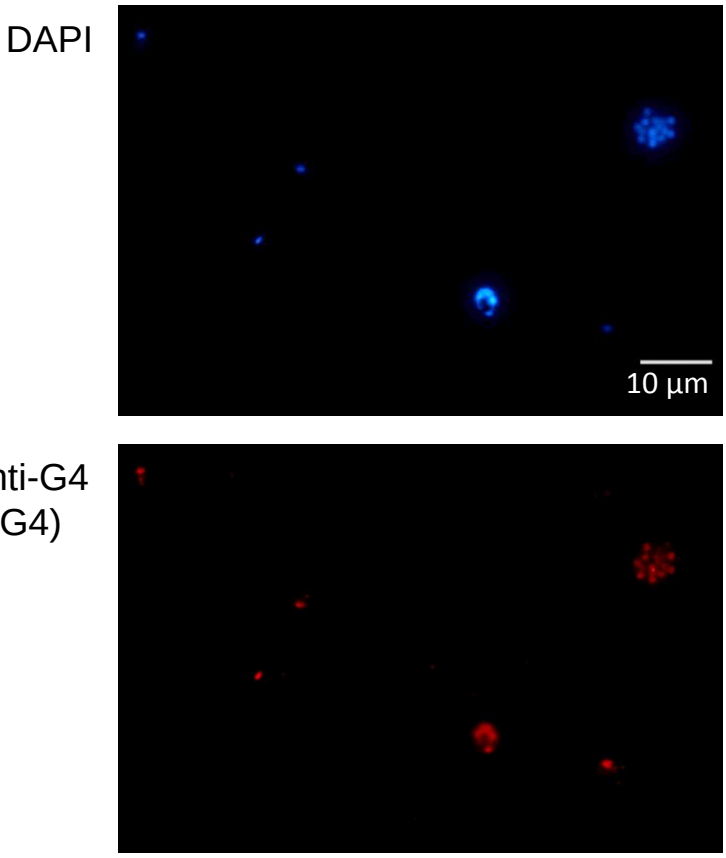

A second independent G-quadruplex-specific antibody detects G-quadruplexes in P. falciparum parasites

Immunofluorescence images showing G-quadruplexes detected with the structure-specific antibody BG4 in *P. falciparum* intraerythrocytic stages (3D7 parasite strain). Images are representative of 2 independent experiments, examining mixed-stage cultures.

Figure S2

A

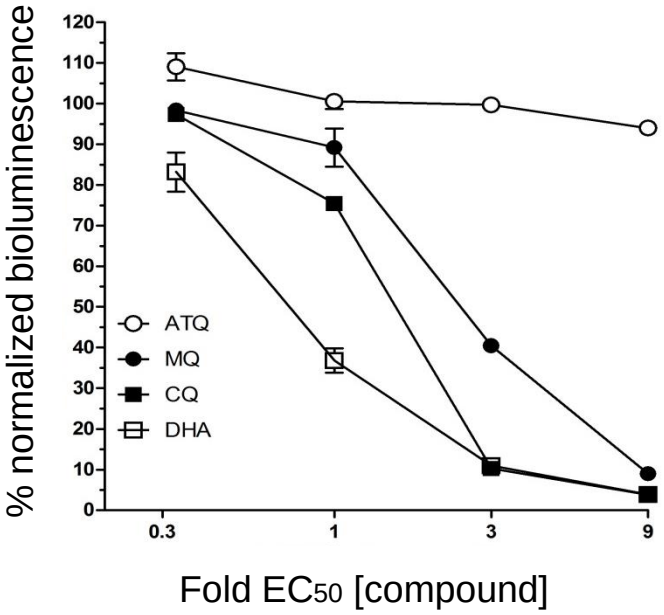

B

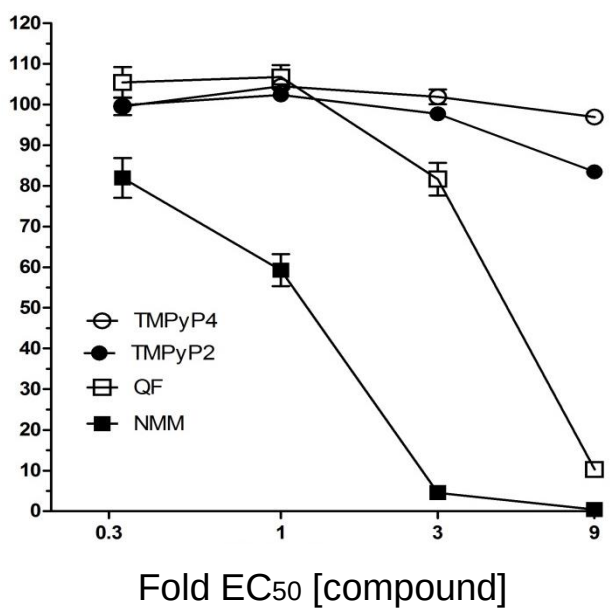

C

Compound	3D7 EC50 (μM)	3D7 95% C.I.	Dd2 EC50 (μM)	Dd2 95% C.I.
QF	0.11	0.108-0.120	0.14	0.133-0.154
TMPyP4	0.62	0.530-0.721	0.52	0.499-0.534
TMPyP2	11.4	8.79-14.9	8.30	7.85-8.77.9

Results of the BRRoK assay in a second parasite strain, NF54, genetically modified with the same luciferase reporter construct as Dd2^{luc}

(A, B) Graphs show the concentration-dependent loss of normalised bioluminescence signal in BRRoK assays against (A) benchmark antimalarials and (B) G-quadruplex-stabilising compounds. The mean bioluminescence signal (normalised against an untreated control) remaining in NF54^{luc} *P. falciparum* after a 6 h exposure to the indicated fold-EC_{50} concentration of each drug or compound is plotted. Error bars represent ±SD from three biological replicates. ATQ, atovaquone; CQ, chloroquine; DHA, dihydroartemisinin; MQ, mefloquine; NMM, N-methyl-mesoporphyrin IX; QF, quarfloxin; TmPyP2, 5,10,15,20-tetra-(N-methyl-2-pyridyl) porphine; TmPyP4, 5,10,15,20-tetra-(N-methyl-4-pyridyl) porphine. Results of this assay in the NF54 background are highly comparable to results in the Dd2 background, shown in Figure 2.

(C) EC_{50} values for several G-quadruplex-binding drugs are shown in both the 3D7 strain (EC_{50} data from Figure 2), which is a clone of NF54, and also in the Dd2 strain, which is the second strain in which the BRRoK assay can be carried out. The mean EC_{50}s from 3 independent Malaria SYBR Green I-based fluorescence (MSF) assays are tabulated and 95% confidence intervals are shown. Mean EC_{50} values for 3D7 and Dd2 are within ~25% of each other in all cases.

Figure S3

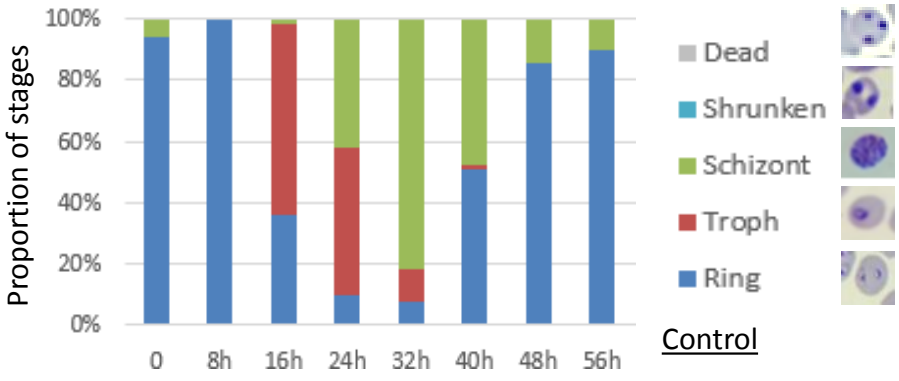

Control

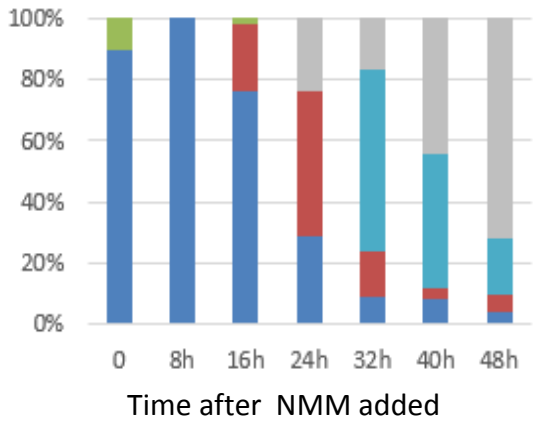

NMM added at rings (0 h)

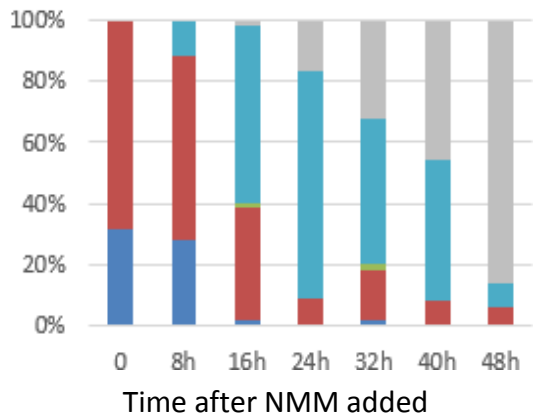

NMM added at trophozoites (16 h)

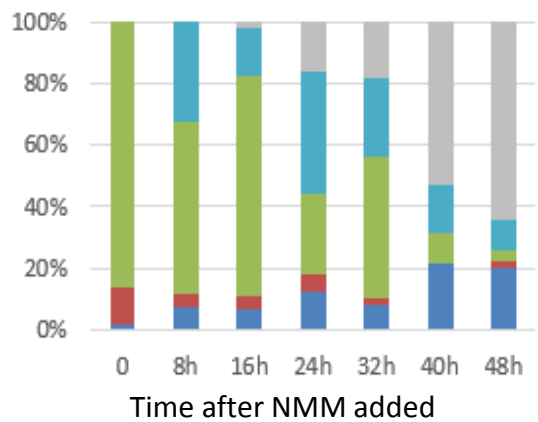

NMM added at schizonts (32 h)

Figure S3: ***NMM is less toxic to ring-stage parasites than to replicative stages***
Developmental stages of 3D7 parasites were assessed at 8 h intervals over a single growth cycle in the absence of any drug, or with NMM added at 130mM (~1.5x EC_{50}) at the ring, trophozoite or schizont stage of the cycle. 50 parasites were counted at each timepoint and photographs show representative parasite morphology at each stage. (Dead parasites stained as a dense intracellular dot without clear morphological features. 'Shrunken' parasites also lacked morphological features but were larger than the completely pyknotic parasites classified as dead. This shrunken stage probably precedes the 'dead' morphology but it can be difficult to distinguish conclusively from the early trophozoite.)

Figure S4

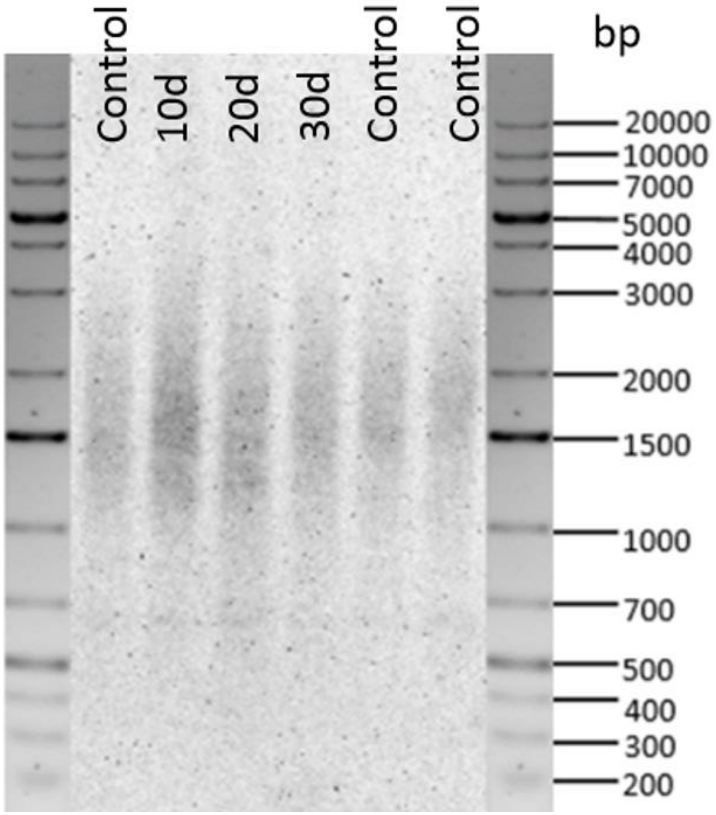

Growth in quarfloxin does not affect telomere maintenance
Telomere restriction fragment (TRF) Southern blot showing telomere lengths in genomic DNA from 3D7 parasites treated for 10, 20 or 30 days with an approximately EC_{50} dose of quarfloxin (120nM). DNA ladders are superimposed either side of the Southern blot.

Figure S5

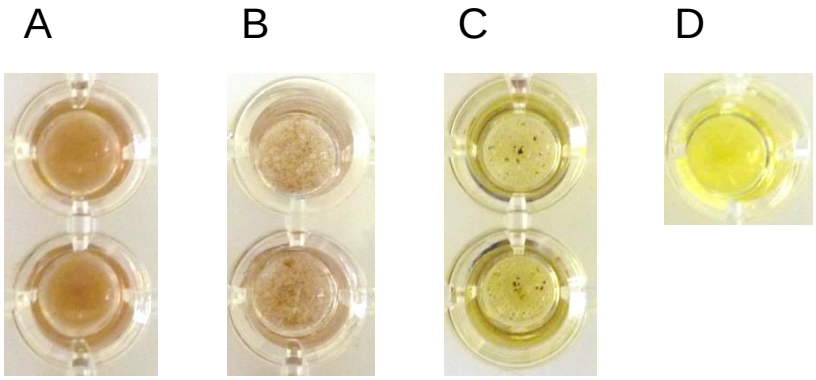

Figure S5: ***Quarfloxin does not inhibit haem crystallisation in vitro***
Results of haem crystallisation assays: (A) at time zero, prior to 4 h incubation with the initiator NP-40 (i.e, negative control), (B) after 4 h incubation with NP-40 (i.e. positive control), (C) after 4 h incubation with NP-40 in the presence of 500mM quarfloxin, (D) 500mM quarfloxin alone, without added haem, showing the drug's strong intrinsic colour.